# Time-dependent model for diluted magnetic semiconductors including band structure and confinement effects

Omar Morandi, Paul-Antoine Hervieux, Giovanni Manfredi

# Time-dependent model for diluted magnetic semiconductors including band structure and confinement effects

O. Morandi,[1,2] P.-A. Hervieux,[2] and G. Manfredi[2]
[1]*INRIA Nancy Grand-Est and Institut de Recherche en Mathématiques Avancées, 7 rue René Descartes, F-67084 Strasbourg, France*
[2]*Institut de Physique et Chimie des Matériaux de Strasbourg, UMR 7504, CNRS, Université de Strasbourg, BP 43, 23 rue du Loess, 67034 Strasbourg Cedex 02, France*

(Received 29 October 2009; revised manuscript received 2 February 2010; published 9 April 2010)

A free-parameter theoretical model is developed in order to study the ultrafast dynamics in confined diluted magnetic semiconductors induced by laser. The hole-spin relaxation process is due to the Elliot-Yafet mechanism, which involves the scattering of the holes on the localized magnetic impurities. The role played by the quantum confinement and the band structure is analyzed. It is shown that the sample thickness and the background hole density strongly influences the phenomenon of demagnetization. Quantitative results are given for III-V ferromagnetic GaMnAs quantum wells of thickness 4 and 6 nm.

DOI: 10.1103/PhysRevB.81.155309 PACS number(s): 78.20.Ls, 78.30.Fs

## I. INTRODUCTION

Ultrafast light-induced magnetization dynamics in ferromagnetic films and in diluted magnetic semiconductors (DMS) is today a very active area of research. Since the observation of the ultrafast dynamics of the spin magnetization in nickel films[1] and the analogous processes in ferromagnetic semiconductors,[2] special interest has been devoted to the development of dynamical models able to mimic the time evolution of the magnetization on both short- and long-time scales. In III-V ferromagnetic semiconductors such as GaMnAs and InMnAs, a small concentration of Mn ions is randomly substituted to cation sites, so that the Mn-Mn spin coupling is mediated by the hole-ion $p-d$ exchange interaction, allowing the generation of a ferromagnetic state with a Curie temperature of the order of 50 K.[3] The magnetism can therefore be efficiently modified by controlling the hole density through doping or by excitation of electron-hole pairs with a laser pulse. In particular, unlike metals, total demagnetization can be achieved in a regime of strong laser excitation.[4]

The time evolution of the total magnetization in wide DMS (layer thickness or the order of $w=70$ nm) excited by laser pulses was presented in Ref. 5. The authors treated the exchange interaction between the holes and the manganese ions in the first quantization formalism and their analysis was performed within a first-order Fermi golden rule (FGR) perturbative framework. In particular, the magnetic ion spin transition rate was evaluated microscopically by means of a balance equation (inverse Overhauser effect) and analogous processes which govern the hole-spin dynamics were taken into account phenomenologically through an equation describing transfer of angular momentum and spin relaxation. In this model, spin relaxation effects are thus included *phenomenologically* by means of a relaxation time which is considered as an adjustable parameter fixed by fitting the experimental measurements.

In the present work, we are interested in developing a parameter-free theoretical model able to describe the out-of-equilibrium dynamical evolution of the hole and magnetic-ion spins in a strongly confined DMS, i.e., ultrathin quantum wells of width smaller than 10 nm. Thus, we have extended the results derived in Ref. 6 by including the band structure of the semiconductor material and a microscopical explanation of the hole-spin relaxation based on the Elliot-Yafet mechanism. The latter involves the scattering of the holes on the localized magnetic impurities of the DMS.

The ultrafast spin relaxation phenomena observed in III-V semiconductors like GaAs, were interpreted by Elliot and Yafet in Ref. 7 as a consequence of a strong spin-orbit (SO) interaction, which is present in wide gap semiconductors. As another consequence of SO, the mixing between heavy and light-hole component of the wave function around the maximum of the hole band leads to an entanglement between the momenta and the spin degrees of freedom. Elliot and Yafet used these considerations to show that a relaxation phenomenon acting on the momentum of a particle such as the phonon scattering by a charge carrier is able to also relax its spin. This mechanism has been studied in a rather general framework in Ref. 8. The study of the Elliot-Yafet mechanism applied to confined semiconductor structures was presented in Ref. 9 and showed that the relaxation time is very sensitive to the Fermi energy of the hole gas and can vary from ps to fs time scale. The same physical assumptions are used in Ref. 10 where an experimental study of the ultrafast demagnetization in $Zn_{1-x}Mn_xSe/Zn_{1-y}Be_ySe$ has been performed. In particular, the authors observe a picosecond time evolution of the magnetization induced by an optical excitation. The experimental findings are interpreted in term of a multiple angular momentum transfer from each spin polarized hole populations to the system of the Mn magnetic ions without change of the hole-spin orientation. An estimate of the relaxation time is obtained within the framework of a first-order perturbation theory and is in agreement with the observed value. In particular, the authors assume that the magnetic ions may be considered in a quasiequilibrium state and the details of the miniband diagram have been discarded.

Let's point out that the spin-orbit interaction plays a very important role in our model. Indeed, our discussion concerning the hole-spin relaxation is manly focused on the effect of this interaction on the spin thermalization. The role of the spin-orbit interaction is rather subtle since, even if it pro-

 

duces the dominant effect it does not enter explicitly in the calculation. The interpretation of the spin relaxation effect is based on the observation that when the parallel momentum of a hole $k_{\|}$ is not strictly zero, the heavy and the light-hole band are mixed together to some extent and the spin projection ceases to be a good quantum number. This effect is taken into account through the *kp* formalism by using the Luttinger-Kohn matrix where the linear momentum appears explicitly and is out-of-diagonal. The physical origin for this band mixing (which is hidden in the *kp* approach) is the spin-orbit interaction which, for example, destroys the degeneracy at the $\Gamma$ point and generates a coupling among different hole states.

Usually a distinction is done between: (i) normal processes for which the Kondo-like scattering between Mn magnetic impurities and holes involves a change in the hole subband (intersub-band process) and (ii) the processes for which initial and final hole states belong to the same sub-band (intrasub-band process).[10] In our approach, both type of processes can qualitatively be explained in the same way: scattering processes that modify the momentum of a particle is able to also modify the spin state of a hole in the presence of a strong spin-orbit interaction. For this reason, in our work, we consider both cases (intrasub-band and intersub-band processes) as different manifestation of the E-Y mechanism.

The paper is organized as follows. In the next section, the theoretical models are described. In Sec. III, numerical results are presented and discussed. Finally, the paper is ended with concluding remarks.

## II. THEORETICAL MODELS

### A. Hole-spin relaxation time: Dynamical simulation

This section is devoted to the modeling of the coherent spin evolution of a hole state interacting with a single Mn impurity. The main contribution to the time evolution of the hole-spin expectation value is due to the exchange interaction

$$V_{\mathrm{ex}} = \gamma \mathbf{M}_{m,m'} \cdot \mathbf{S}_{s,s'} \quad \delta(\mathbf{R}_\eta - \mathbf{r}), \tag{1}$$

where $\gamma$ is the exchange coupling constant and $\mathbf{r}$ ($\mathbf{S}$), $\mathbf{R}_\eta$ ($\mathbf{M}$) are, respectively, the position (spin matrix) of the hole and ion. Hereafter, the spin operators corresponding to the $\mathbf{S}$ and $\mathbf{M}$ matrices will be denoted by $\mathcal{S}$ and $\mathcal{M}$, respectively. The exchange interaction factors into two terms acting, respectively, on the spatial and the spin degrees of freedom. In particular, the term $\mathbf{M}_{m,m'} \cdot \mathbf{S}_{s,s'}$ conserves the total spin of the system allowing for a transfer of spin angular momentum between the holes and the magnetic ions. The leak of ion spin polarization is compensated by an equal rising of the spin polarization of the hole gas. The term $\delta(\mathbf{R}_\eta - \mathbf{r})$ acts only on the spatial degrees of freedom and is responsible for the change of the linear momentum of the scattered particle. Elliot and Yafet have observed that, when the spin projection is not a good quantum number, as it is the case for a hole state in a semiconductor alloy, any interaction which scatters a particle from a linear momentum $k$ to $k'$ will also affect the hole spin with a consequent probability of modifying its spin direction.[7] We conclude that, since the exchange interaction changes both the spin and the linear momentum of the hole, it can be responsible for the relaxation of the total hole spin in the same way as the phonon scattering process does.

We illustrate our conclusions with the following simple example. For the sake of simplicity, we here refer to the special case of a spherical symmetry of the band diagram. Our conclusions are independent on this approximation that will be not used in the next sections. The *kp* Hamiltonian $\mathcal{H}_{kp}$ of a hole in a uniform semiconductor bulk structure is a $n \times n$ matrix (where $n$ is the total number of bands) parametrized by the quasi-momentum $\mathbf{k}$ of the particle. As it is well known, for $\mathbf{k}=0$, $\mathcal{H}_{kp}$ is diagonal and therefore the band eigenstates are also spin eigenstates. For $t=t_0$ we consider a hole in a $n$-th $\mathbf{k}=0$ eigenstate, and we denote its wave function by $\xi_n(\mathbf{k},t_0)=\varphi_n \delta(\mathbf{k})$ with $\mathcal{H}_{kp}(\mathbf{0})\varphi_n = \varepsilon_{\mathbf{0},n}\varphi_n$ where $\varepsilon_{\mathbf{k},n}$ are the eigenvalues of $\mathcal{H}_{kp}(\mathbf{k})$. Under the action of the exchange interaction of Eq. (1) the particle is scattered from $\mathbf{k}=0$ to a superposition of states with different momenta. According to the Elliot-Yafet mechanism, when the states with $\mathbf{k} \neq 0$ start to be populated the hole spin starts to precess. For the sake of simplicity we consider a single scattering event where, for example, the hole spin is lowered by one unit of angular momentum thanks to the operator $\mathcal{M}^+\mathcal{S}^-$ and its momentum becomes $\mathbf{k}_0$ (the following considerations can be easily extended to a superposition of states). The spin component of the state $\xi_n' = \mathcal{S}^- \xi_n$ is no more an eigenstate of $\mathcal{H}_{kp}(\mathbf{k}_0)$ and its time evolution can be easily estimated by a projection over the spin eigenstates $\xi_{n_1}(\mathbf{k}_0)$ of $\mathcal{H}_{kp}(\mathbf{k}_0)$. In particular, the hole-spin expectation value with respect to a given direction $\hat{\mathbf{n}}$ reads

$$\langle \xi_n' | \hat{\mathbf{n}} \cdot \mathcal{S} | \xi_n' \rangle = \sum_{n_1,n_2} \langle \xi_{n_1}(\mathbf{k}_0) | \hat{\mathbf{n}} \cdot \mathcal{S} | \xi_{n_2}(\mathbf{k}_0) \rangle \langle \xi_{n_2}(\mathbf{k}_0) | \xi_n' \rangle \times \langle \xi_n' | \xi_{n_1}(\mathbf{k}_0) \rangle e^{i/\hbar(\varepsilon_{\mathbf{k}_0,n_1} - \varepsilon_{\mathbf{k}_0,n_2})(t-t_0)}. \tag{2}$$

A theoretical study shows that, in the spherical approximation of the band diagram, for any $\mathbf{k}_0$ it is always possible to find a direction $\hat{\mathbf{n}}_{\mathbf{k}_0}$ for which the spin of the hole eigenvector $\xi_{n_1}(\mathbf{k}_0)$ is oriented along $\hat{\mathbf{n}}_{\mathbf{k}_0}$.[11] It is immediate to verify that only the spin component of $\xi_n'$ along $\hat{\mathbf{n}}_{\mathbf{k}_0} \neq \hat{\mathbf{z}}$ is stationary while the perpendicular component oscillates with a frequency of the order of $\omega \propto (\varepsilon_{\mathbf{k}_0,n_1} - \varepsilon_{\mathbf{k}_0,n_2})/\hbar$. In a semiconductor device like a DMS, the quantum confinement of the hole gas can give rise to a strong splitting of the energy levels and consequently the oscillation frequencies $\omega$ can induce a non-negligible relaxation of the $z$ projection of the hole spin (some numerical simulations concerning the stationary states of a 4–6 nm DMS will be presented in Sec. III). In our discussion we have simplified the spin dynamics by assuming a single hole-ion scattering event (which is in the spirit of a first-order Dyson expansion). Generally, the linear momentum of the hole is continuously modified by the Dirac delta function and the previous approximation holds when the scattering frequency is lower than the rotation frequency $\omega$.

These considerations can be verified with the following numerical model. We consider the time evolution of the hole wave function in the presence of the impurity magnetic field

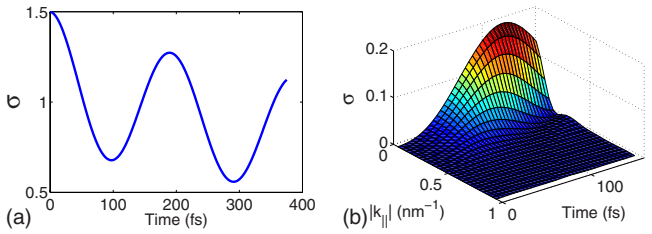


FIG. 1. (Color online) (a) $\sigma$ (see text for the definition) as a function of time for $|\mathbf{k}_\parallel|=0$. (b) $\sigma$ as a function of $|\mathbf{k}_\parallel|>0$ and time.

in the single-particle approximation. In particular we are interested in the study of the spin evolution in a strongly confined DMS (magnetic layer thickness of the order of a few nm). According to the $kp$ theory the evolution equation for the hole envelope function is

$$i\hbar\frac{\partial\tilde{\xi}_n(\mathbf{r},t)}{\partial t}=\sum_{n'}\left[\mathcal{H}_{kp}\left(\frac{\partial}{\partial\mathbf{r}_\parallel},\frac{\partial}{\partial z}\right)\right]_{n,n'}\tilde{\xi}_{n'}(\mathbf{r},t)+\gamma\sum_{n',\eta}\mathbf{M}_{\mathbf{R}_\eta}\cdot\mathbf{S}_{n,n'}\delta(\mathbf{r}-\mathbf{R}_\eta)\tilde{\xi}_{n'}(\mathbf{r},t).$$

By using $\xi_n(\mathbf{k}_\parallel,z,t)=\int\tilde{\xi}_n(\mathbf{r},t)e^{-i\mathbf{k}_\parallel\cdot\mathbf{r}_\parallel}\mathrm{d}\mathbf{r}_\parallel$, we obtain

$$i\hbar\frac{\partial\xi_n(\mathbf{k}_\parallel,z,t)}{\partial t}=\sum_{n'}\left[\mathcal{H}_{kp}\left(\mathbf{k}_\parallel,\frac{\partial}{\partial z}\right)\right]_{n,n'}\xi_{n'}(\mathbf{k}_\parallel,z,t)+\frac{\gamma}{4\pi^2}\mathbf{M}^z(z)\mathbf{S}^z_{n,n}\int\xi_n(\mathbf{k}'_\parallel,z,t)\mathrm{d}\mathbf{k}'_\parallel,$$

where the $z$ axis is the quantization direction, $\mathbf{M}^z_{\mathbf{R}_\eta}\equiv\mathrm{Tr}(\mathcal{M})=\Sigma_m\langle\mathbf{R}_\eta;m|\mathcal{M}|\mathbf{R}_\eta;m\rangle$ denotes the spin of the ion located in $\mathbf{R}_\eta$ with a magnetization directed along the $z$ axis. Furthermore, we have used the following approximations: $\mathbf{M}^z_{\mathbf{k}_\parallel}=\Sigma_{\mathbf{R}^\parallel_\eta}\mathbf{M}_{\mathbf{R}^\parallel_\eta}(z)e^{i\mathbf{k}_\parallel\cdot\mathbf{R}^\parallel_\eta}\simeq\mathbf{M}^z$ and the $\mathbf{k}_\parallel$ dependence of $\mathbf{M}$ has been discarded. Due to the presence of the delta function in the above equation, we have $\mathbf{R}^z_\eta=z$ and $\mathcal{M}$ is the ion spin operator.

It is easy to show that if the Hamiltonian is axially symmetric with respect to the $z$ axis and if the initial condition for $\xi_n$ depends only on the modulus of $\mathbf{k}_\parallel$, then the solution at any time will also only depend on $|\mathbf{k}_\parallel|$, leading to

$$i\hbar\frac{\partial\xi_n(\mathbf{k}_\parallel,z,t)}{\partial t}=\sum_{n'}\left[\mathcal{H}_{kp}\left(\mathbf{k}_\parallel,\frac{\partial}{\partial z}\right)\right]_{n,n'}\xi_{n'}(\mathbf{k}_\parallel,z,t)+\frac{\gamma}{2\pi}\mathbf{M}^z(z)\mathbf{S}^z_{n,n}\int\xi_n(\mathbf{k}'_\parallel,z,t)\mathrm{d}|\mathbf{k}'_\parallel|.$$

In Fig. 1, the numerical solution of the above equation is shown by taking the initial condition $\xi_n(\mathbf{k}_\parallel,z,t_0)=4\pi^2\delta(\mathbf{k}_\parallel)\varphi_n^{+3/2}(z)$ where the functions $\varphi_n^m$ are solutions of

$$\sum_{n'}\left[\mathcal{H}_{kp}\left(\mathbf{0},\frac{\partial}{\partial z}\right)\right]_{n,n'}\varphi^m_{n'}=\varepsilon^m\varphi^m_n\quad m=\pm 3/2;\pm 1/2. \tag{3}$$

In particular, the quantity $\sigma=\Sigma_n\int|\xi_n(\mathbf{k}_\parallel,z,t)|^2\mathrm{d}z$ for $|\mathbf{k}_\parallel|=0$ [Fig. 1(a)] and for $|\mathbf{k}_\parallel|>0$ [Fig. 1(b)] is depicted as a function of time. The numerical solution shows that, on a time scale of the order of 100 fs, as a consequence of the hole-ion local scattering, the component with non vanishing quasimomentum of the solution starts to be populated and the initial coherence of spin of the particle is lost. The expectation value the $z$ component of the spin is thus mediated over the states with $|\mathbf{k}_\parallel|>0$ where the expectation value is smaller than 1.5.

### B. Dynamical modeling of the exchange interaction

This section is devoted to a deeper investigation of the hole-spin relaxation effects induced by the exchange interaction. We consider the simplest case of a two-particle system constituted of a single hole interacting with one Mn impurity. The effect of the other magnetic ions is modeled by an effective magnetic potential $\mathbf{H}_{mf}$ acting on the hole (mean-field approximation). The total Hamiltonian is therefore

$$\mathcal{H}=\mathcal{H}_{kp}+\mathcal{H}_{mf}+\mathcal{V}_{\mathrm{ex}}, \tag{4}$$

where the Luttinger-Kohn Hamiltonian $\mathcal{H}_{kp}$ describes the effect of the lattice. The exchange interaction is

$$\mathcal{V}_{\mathrm{ex}}=\gamma\mathcal{M}\cdot\mathcal{S}\delta(\mathbf{r}-\mathbf{R}_\eta), \tag{5}$$

where $\mathcal{S}$ and $\mathcal{M}$ are the spin operators acting on the Hilbert space of the holes and ions, respectively. The exchange interaction shows that the natural Hilbert space where to perform the theoretical study of the system is

$$\mathbb{H}^1=\mathbb{H}_{\mathrm{h}}\otimes\mathbb{H}_{\mathrm{Mn}}, \tag{6}$$

where $\mathbb{H}_{\mathrm{h}}$ and $\mathbb{H}_{\mathrm{Mn}}$ are the Hilbert space of the holes and ions, respectively. The wave function of the system is

$$\Psi(\mathbf{r},s;\mathbf{R}_\eta,m)=\langle\mathbf{r},s;\mathbf{R}_\eta,m||\mathrm{h}\rangle\otimes|\mathrm{Mn}\rangle, \tag{7}$$

where $|\mathrm{h}\rangle(|\mathrm{Mn}\rangle)$ is the component of the hole (ion) wave function in the Dirac formalism. $\mathbf{r}$ ($\mathbf{R}_\eta$) and $s$ ($m$) are the spatial coordinates and spin projections of the holes (ions). The Schrödinger equation for $\Psi$ takes into account all the coherent correlations between holes and ions. The formulation of the problem in the Hilbert space $\mathbb{H}^1$ requires a great numerical effort even for solving the simple two-particle problem. This is due to the complete mixing of the spatial degrees of freedom and those pertaining to the hole and ion spins (because generally the total wave function does not factor into a product of the holes and ions wave functions). The usual way to circumvent this difficulty is to project the solution in the Hilbert space

$$\mathbb{H}^2=\mathbb{H}_{\mathrm{h}}\oplus\mathbb{H}_{\mathrm{Mn}}. \tag{8}$$

In this approximation, the dimensionality of the problem reduces from $\dim(\mathbb{H}_{\mathrm{h}})\times\dim(\mathbb{H}_{\mathrm{Mn}})$ to $\dim(\mathbb{H}_{\mathrm{h}})+\dim(\mathbb{H}_{\mathrm{Mn}})$. We formally define the projection operator $\mathcal{P}^{\mathrm{h}}$ and the analogous $\mathcal{P}^{\mathrm{Mn}}$ as

$$\mathcal{P}^{\mathrm{h}}\mathcal{O} = \mathrm{Tr}_{\mathrm{Mn}}\{\mathcal{O}\}, \tag{9}$$

where $\mathcal{O}$ is a generic operator acting on $\mathbb{H}^1$ and $\mathrm{Tr}_{\mathrm{Mn}}$ denotes the partial trace with respect the ion spin degrees of freedom. In particular, we have

$$\mathcal{P}^{\mathrm{h}}\mathcal{V}_{\mathrm{ex}} = \gamma\delta(\mathbf{r}-\mathbf{R}_\eta)\langle\mathbf{M}\rangle\cdot\mathcal{S}, \tag{10}$$

$$\mathcal{P}^{\mathrm{Mn}}\mathcal{V}_{\mathrm{ex}} = \gamma\delta(\mathbf{r}-\mathbf{R}_\eta)\langle\mathbf{S}\rangle\cdot\mathcal{M}, \tag{11}$$

where $\langle\mathbf{M}\rangle$ and $\langle\mathbf{S}\rangle$ are, respectively, the expectation value of the ion and hole spin.

We point out that the reduction in the dimensionality of the problem may cause a misleading interpretation of the spin dynamics induced by the exchange operator. We illustrate the limitations of this approximation procedure with the following example. For the sake of simplicity, we assume that the total spin of both the holes and the ions is $\mathfrak{S}^M = \mathfrak{S}^h = 1/2$ and we focus our attention on the spin degrees of freedom of $\mathcal{V}_{\mathrm{ex}}$. For the following discussion, we consider the simplified exchange interaction (we set $\gamma=1$)

$$\mathcal{V}'_{\mathrm{ex}} = \mathcal{M}\cdot\mathcal{S}. \tag{12}$$

In $\mathbb{H}^1$ the hole-ion system is defined by the density matrix $\rho^2(t) = [|\mathrm{h}(t)\rangle\otimes|\mathrm{Mn}(t)\rangle][\langle\mathrm{h}(t)|\otimes\langle\mathrm{Mn}(t)|]$ $= |\mathrm{h}(t);\mathrm{Mn}(t)\rangle\langle\mathrm{h}(t);\mathrm{Mn}(t)|$. In $\mathbb{H}^2$, the *a priori* decoupling of the spin degrees of freedom of the holes with respect to those of the ions allows us to define two density matrices: $\rho^2_{\mathrm{h}}(t) = |\mathrm{h}(t)\rangle\langle\mathrm{h}(t)|$ and $\rho^2_{\mathrm{Mn}}(t) = |\mathrm{Mn}(t)\rangle\langle\mathrm{Mn}(t)|$. The evolution of $\rho^2$ is

$$i\frac{\partial\rho^2_{\mathrm{h}}}{\partial t} = [\langle\mathbf{M}\rangle\cdot\mathcal{S}, \rho^2_{\mathrm{h}}], \tag{13}$$

$$i\frac{\partial\rho^2_{\mathrm{Mn}}}{\partial t} = [\langle\mathbf{S}\rangle\cdot\mathcal{M}, \rho^2_{\mathrm{Mn}}], \tag{14}$$

where $\langle\mathbf{M}\rangle$ can be expressed in term of $\rho^2_{\mathrm{Mn}}$: $\langle\mathbf{M}\rangle = \mathrm{Tr}\{\mathcal{M}\rho^2_{\mathrm{Mn}}\}$. In this section for sake of simplicity we pose $\hbar=1$. It is easy to see that Eqs. (13) and (14) are equivalent to

$$\frac{\partial\langle\mathbf{S}\rangle}{\partial t} = \langle\mathbf{S}\rangle\wedge\langle\mathbf{M}\rangle, \tag{15}$$

$$\frac{\partial\langle\mathbf{M}\rangle}{\partial t} = \langle\mathbf{M}\rangle\wedge\langle\mathbf{S}\rangle. \tag{16}$$

It is not possible to derive Eq. (13) from the exact equation of motion of $\rho^1$ in $\mathbb{H}^1$

$$i\frac{\partial\rho^1}{\partial t} = [\mathcal{H}'_{\mathrm{ex}}, \rho^1]. \tag{17}$$

In fact, if we apply the projection operator to the previous equation and identify $\rho^2_{\mathrm{h}} = \mathcal{P}^{\mathrm{h}}\rho^1$, $\rho^2_{\mathrm{Mn}} = \mathcal{P}^{\mathrm{Mn}}\rho^1$, in order to obtain Eq. (13) we need the following approximation:

$$\mathcal{P}^{\mathrm{h}}(\mathcal{V}'_{\mathrm{ex}}\rho^1) \simeq \mathcal{P}^{\mathrm{h}}(\mathcal{V}'_{\mathrm{ex}})\mathcal{P}^{\mathrm{h}}(\rho^1). \tag{18}$$

If one solves Eqs. (15) and (16) using an initial condition where the hole spin is antiparallel to the ion spin (i.e., $\rho^2_{\mathrm{h}}(t_0) = |\uparrow\rangle\langle\uparrow|$ and $\rho^2_{\mathrm{Mn}}(t_0) = |\downarrow\rangle\langle\downarrow|$ the $z$ axis being the quantization direction) one obtains

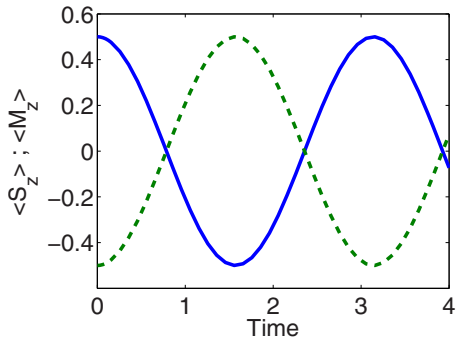


FIG. 2. (Color online) Projection along the $z$ axis of the hole spin (full line), and ion spin (dashed line) as a function of time (the time is normalized in unit of $\hbar/\gamma$).

$$\langle\mathbf{M}\rangle(t) = \langle\mathbf{M}\rangle(t_0) = -\frac{1}{2}\hat{\mathbf{z}}, \tag{19}$$

$$\langle\mathbf{S}\rangle(t) = \langle\mathbf{S}\rangle(t_0) = \frac{1}{2}\hat{\mathbf{z}}. \tag{20}$$

In contrast to what was expected, the exchange interaction in the reduced Hilbert space does not induce any spin rotation. On the other hand Eq. (17) leads to a non trivial dynamics. This can be seen by writing the exchange interaction in the canonical basis of $\mathbb{H}^1$ where the wave vector is represented by

$$\Psi = \begin{pmatrix} \psi(s=\uparrow, m=\uparrow) & s=\uparrow \\ \psi(s=\downarrow, m=\uparrow) & s=\downarrow \\ \psi(s=\uparrow, m=\downarrow) & s=\uparrow \\ \psi(s=\downarrow, m=\downarrow) & s=\downarrow \end{pmatrix} \begin{matrix} \\ \\ \}m=\uparrow \\ \}m=\downarrow \end{matrix} \qquad \Psi(t_0) = \begin{pmatrix} 0 \\ 0 \\ 1 \\ 0 \end{pmatrix},$$

$$\mathcal{V}_{\mathrm{ex}} = \begin{pmatrix} 1/4 & 0 & 0 & 0 \\ 0 & -1/4 & 1 & 0 \\ 0 & 1 & -1/4 & 0 \\ 0 & 0 & 0 & 1/4 \end{pmatrix}.$$

In Fig. 2, we present the expectation value of the ion spin given by $\langle\mathbf{M}\rangle = \mathrm{Tr}_{\mathrm{Mn}}\{\mathcal{M}\mathcal{P}^{\mathrm{Mn}}\rho^1\}$ where $\rho^1$ is the numerical solution of Eq. (17). Let us note that, since to a pure-state solution in $\mathbb{H}^1$ corresponds a mixed-state solution in the reduced Hilbert space $\mathbb{H}^2$, the modulus of $\langle\mathbf{M}\rangle$ is no more constant. The aim of the above discussion was to reveal the modeling error that is made when the full dynamical correlation between hole and ion spins is discarded.

In Sec. II A, we estimated the hole-spin relaxation time by neglecting the exchange interaction. Indeed, this is due to the assumption that the hole-spin dispersion comes from (i) the Dirac delta function in the exchange Hamiltonian, and (ii) the spin-orbit interaction which entangles the linear momentum and the spin projection of the holes. When a hole is scattered by the hard-core potential represented by the Dirac delta function, all the values of the outgoing quasimomentum

are excited and therefore a fast dispersion of the spin projection is expected even in the absence of an exchange of spin angular momentum between the holes and the ions. In presence of this scattering regime, the long-time correlation between the spin of the holes and that of the ions can be discarded and we can set the dynamics in the Hilbert space $\mathbb{H}^2$ where the spin correlation is averaged out by the projection procedure described in this section. Furthermore we remark that in Sec. II A we have discarded the fluctuations of the mean spin polarization of the ions induced by the presence of the hole. In particular, the terms $\mathcal{M}^{\pm}\mathcal{S}^{\mp}$ describe a two-particle interaction where both the hole spin and the ion spin are modified. They cannot be included in the single-particle approximation used to derive the equation of motion and a static concentration of the background ion spin can thus be assumed. The full interaction $\mathcal{M}\cdot\mathcal{S}$ is restored in the next paragraph where we have applied an approach based on the Fermi golden rule for describing the dynamics in a confined DMS including both *the spin polarization flux and the hole-spin relaxation.*

### C. Time evolution of the total magnetization in confined DMS

We derive the time evolution equations for the hole and ion densities in the first quantization formalism and within the framework of the first-order FGR approximation. The exchange interaction $\mathcal{V}_{\rm ex}^{\eta}=\gamma\mathcal{M}\cdot\mathcal{S}\delta(\mathbf{R}_{\eta}-\mathbf{r})$ is treated as a perturbation. We define the normalized hole and ion densities $n_{\mathbf{s}}$ and $\mathfrak{n}_m$ as,

$$n_{\mathbf{s}}=\frac{1}{N^S}\sum_{\mathbf{k}_{\parallel}} n_{\mathbf{k}_{\parallel},\mathbf{s}}, \tag{21}$$

$$\mathfrak{n}_m=\frac{1}{N^M}\sum_{\eta}\mathfrak{n}_{\eta,m}, \tag{22}$$

where $n_{\mathbf{k}_{\parallel},\mathbf{s}}$, $\mathfrak{n}_{\eta,m}$ are, respectively, the hole and ion occupation probability and $\mathbf{k}_{\parallel}$ is the transverse momentum which lies in the plane of the quantum well. $N^S$ and $N^M$ are the total density of holes and ions, respectively, and $m$ denotes the $z$ projection of the ion spin, $\mathbf{s}=(s,b)$ where $s$ and $b$ are, respectively, the band and sub-band index. The latter enumerates bound states in the $z$ direction (the periodicity of the total Hamiltonian is lost along the $z$ axis). For the light and heavy hole states $s=\pm 3/2,\pm 1/2$, each band is labeled with the corresponding spin at the $\Gamma$ point (which is still, for $\mathbf{k}_{\parallel}\neq 0$, the main contribution to the spin projection). The time evolution equations read

$$\frac{\partial n_{\mathbf{s}}}{\partial t}=\frac{1}{N^S}\sum_{m}\mathcal{W}_{\mathbf{s},m}, \tag{23}$$

$$\frac{\partial \mathfrak{n}_m}{\partial t}=\frac{1}{N^M}\sum_{\mathbf{s}_i}\mathcal{W}_{\mathbf{s}_i,m}, \tag{24}$$

$$\mathcal{W}_{\mathbf{s}_i,m}=N^M\frac{2\pi}{\hbar}\sum_{\mathbf{k}_{i\parallel},\mathbf{k}_{f\parallel},\mathbf{s}_f}\sum_{m'}|\tilde{\mathcal{V}}_{i\to f}|^2[\mathfrak{n}_{m'}n_{\mathbf{k}_{f\parallel},\mathbf{s}_f}(1-n_{\mathbf{k}_{i\parallel},\mathbf{s}_i}) - \mathfrak{n}_m n_{\mathbf{k}_{i\parallel},\mathbf{s}_i}(1-n_{\mathbf{k}_{f\parallel},\mathbf{s}_f})]\delta(E_i-E_f), \tag{25}$$

where $E_i=\varepsilon_{\mathbf{k}_{i\parallel},\mathbf{s}_i}+E_m$ $(E_f=\varepsilon_{\mathbf{k}_{f\parallel},\mathbf{s}_f}+E_{m'})$ is the initial (final) total energy. $E_m$ is the energy of the $m^{\rm th}$ ionic level and $\varepsilon_{\mathbf{k}_{\parallel},\mathbf{s}}$ is defined below in Eq. (26). $\mathcal{V}_{i\to f}^{\eta}\equiv\mathcal{V}_{\mathbf{k}_{i\parallel},\mathbf{s}_i,m\to\mathbf{k}_{f\parallel},\mathbf{s}_f,m'}^{\eta}=\langle\psi_{\mathbf{k}_{i\parallel},\mathbf{s}_i},m|\mathcal{V}_{\rm ex}^{\eta}|\psi_{\mathbf{k}_{f\parallel},\mathbf{s}_f},m'\rangle$ is the usual matrix element of the scattering rate and describes the transition probability between two scattering hole states $\psi_{\mathbf{k}_{\parallel},\mathbf{s}}$ with a simultaneous ion spin transition $(m\to m')$. In order to derive Eqs. (23)–(25), we have assumed that for a given regular function $f(\eta)$, the following homogeneous approximation holds for the ion spatial degrees of freedom:[12]

$$\sum_{\eta}|\mathcal{V}_{i\to f}^{\eta}|^2 f(\eta)\simeq\frac{1}{V}\int_V|\mathcal{V}_{i\to f}^{\eta}|^2 d\mathbf{R}_{\eta}\sum_{\eta}f(\eta)=|\tilde{\mathcal{V}}_{i\to f}|^2\sum_{\eta}f(\eta).$$

We have applied the *kp* theory for evaluating the scattering states $\psi_{\mathbf{k}_{\parallel},\mathbf{s}}(\mathbf{r})$ for a confined heterostructure. In a bulk semiconductor, the scattering states coincide with the Bloch wave functions $\psi_{\mathbf{k},n}^B(\mathbf{r})=e^{i\mathbf{k}\cdot\mathbf{r}}u_{\mathbf{k},n}(\mathbf{r})$.

The *kp* theory assumes that, when the lattice translational symmetry is broken along a given direction, as it is the case for a confined DMS, the periodic part of the Bloch function $u_{\mathbf{k},\mathbf{s}}$ can be considered to be nearly the same for all the heterostructure, and the spatial variation of the band diagram can be modeled by introducing a smooth variation of the parameters characterizing the bulk structure in the $z$ direction. In the problem we are concerned with, the scattering wave functions $\psi_{\mathbf{k}_{\parallel},\mathbf{s}}(\mathbf{r})$ are the eigenstates of the DMS heterostructure

$$\left(-\frac{\hbar^2\Delta}{2m_0}+V_p(\mathbf{r})+V_{\rm np}(\mathbf{r})+V_Z(\mathbf{r})\right)\psi_{\mathbf{k}_{\parallel},\mathbf{s}}(\mathbf{r})=\varepsilon_{\mathbf{k}_{\parallel},\mathbf{s}}\psi_{\mathbf{k}_{\parallel},\mathbf{s}}(\mathbf{r}), \tag{26}$$

where $m_0$ is the electron mass, $V_p(\mathbf{r})$ is the periodic lattice potential and $V_{\rm np}(\mathbf{r})$ is a nonperiodic external potential, which takes into account different effects like: (i) the bias voltage applied across the device; (ii) the contribution coming from the doping impurities; (iii) the self-consistent field produced by the mobile electronic charge carriers. $V_Z(\mathbf{r})$ is the Zeeman contribution which is calculated self-consistently from the hole-spin density as in the Zener model.[13]

Expansion of $\psi_{\mathbf{k}_{\parallel},\mathbf{s}}(\mathbf{r})$ on the basis of the Kane *kp* functions reads

$$\psi_{\mathbf{k}_{\parallel},\mathbf{s}}(\mathbf{r})=\sum_{n'}u_{\mathbf{0},n'}(\mathbf{r})\tilde{\varphi}_{n'}^{\mathbf{k}_{\parallel},\mathbf{s}}(\mathbf{r}).$$

The envelope functions, $\tilde{\varphi}_{n'}^{\mathbf{k}_{\parallel},\mathbf{s}}(\mathbf{r})$, are solutions of the Kane Hamiltonian system

$$\sum_{n'}\left[\mathcal{H}_{kp}\left(\mathbf{k}'_{\parallel},\frac{\partial}{\partial z}\right)\right]_{n,n'}\varphi_{n'}^{\mathbf{k}_{\parallel},\mathbf{s}}(\mathbf{k}'_{\parallel},z)=\varepsilon_{\mathbf{k}_{\parallel},\mathbf{s}}\varphi_{n}^{\mathbf{k}_{\parallel},\mathbf{s}}(\mathbf{k}'_{\parallel},z),\quad(27)$$

where $\varphi_n^{\mathbf{k}_\parallel,\mathbf{s}}(\mathbf{k}'_\parallel,z)\equiv\frac{1}{2\pi}\int\tilde{\varphi}_n^{\mathbf{k}_\parallel,\mathbf{s}}(\mathbf{r})e^{-i\mathbf{k}'_\parallel\cdot\mathbf{r}}\mathrm{d}\mathbf{k}'_\parallel$ and can be written as $\varphi_n^{\mathbf{k}_\parallel,\mathbf{s}}(\mathbf{k}'_\parallel,z)=\delta(\mathbf{k}_\parallel-\mathbf{k}'_\parallel)\chi_n^{\mathbf{k}_\parallel,\mathbf{s}}(z)$ where the functions $\chi_n^{\mathbf{k}_\parallel,\mathbf{s}}(z)$ are solutions of the system

$$\sum_{n'}\left[\mathcal{H}_{kp}\left(\mathbf{k}_{\parallel},\frac{\partial}{\partial z}\right)\right]_{n,n'}\chi_{n'}(z)=\varepsilon_{\mathbf{k}_\parallel,\mathbf{s}}\chi_n(z).\quad(28)$$

We note that care has to be taken to obtain a correct modeling of the boundary conditions in the envelope *kp* approach.[14] Indeed, in the envelope function approximation, the inhomogeneity of the system is commonly taken into account by considering bulk band parameters which vary discontinuously at the interfaces. In this approach, microscopic effects due to the interfaces are neglected and, in particular, the periodic part of the Bloch's function is considered nearly unaffected by their presence. Despite the fact that discontinuous band parameters go beyond the range of validity of the envelope function approximation, it has been observed that such an ansatz is capable of describing electron and hole states in quantum wells in a very good agreement with experiment (for a general discussion of this point see Refs. 11 or 15 for the case of "nasty" discontinuity).

More specifically, in our model we have followed the same procedure as the one given in Ref. 16 or in Ref. 12. Since we restrict ourselves to the Luttinger-Kohn Hamiltonian, spurious solutions that could affect a general Kane model do not occur.[11]

If $\mathcal{S}$ is an operator acting on the hole-spin Hilbert space, we have

$$\mathcal{S}|\mathbf{0},n\rangle^P=S(n)|\mathbf{0},\tilde{S}(n)\rangle^P,$$

where $u_{\mathbf{k},n}(\mathbf{r})=\langle\mathbf{r}|\mathbf{k},n\rangle^P$. For example, for the heavy or light-hole band (where $n=\pm3/2;\pm1/2$) the raising-lowering operator $\mathcal{S}^\pm$ gives

$$\mathcal{S}^\pm|\mathbf{0},n\rangle^P=\sqrt{(\mathfrak{S}^h\mp n)(\mathfrak{S}^h\pm n+1)}|\mathbf{0},n\pm1\rangle^P,$$

where $\mathfrak{S}^h$ is the total angular momentum of the holes and

$$\langle\mathbf{r}|\mathcal{S}|\mathbf{k},\mathbf{n}\rangle=\sum_{n'}S(n')\tilde{\varphi}_{n'}^{\mathbf{k},\mathbf{n}}(\mathbf{r})u_{\mathbf{0},\tilde{S}(n')}(\mathbf{r}),$$

where $\langle\mathbf{r}|\mathbf{k},\mathbf{n}\rangle=\psi_{\mathbf{k},\mathbf{n}}(\mathbf{r})$. The scattering matrix element becomes

$$\begin{aligned}\mathcal{V}^\eta_{\mathbf{k}_\parallel,\mathbf{s},m\to\mathbf{k}_{1\parallel},\mathbf{s}_1,m'}&=\gamma\langle m|\mathcal{M}^\pm|m'\rangle\langle\mathbf{k}_\parallel,\mathbf{s}|\delta(\mathbf{r}-\mathbf{R}_\eta)\mathcal{S}^\mp|\mathbf{k}_{1\parallel},\mathbf{s}_1\rangle\\&=\gamma\mathbf{M}^\pm_{m,m'}\sum_{n_1,n_2}S^\mp(n_2)\int\bar{\tilde{\varphi}}_{n_1}^{\mathbf{k}_\parallel,\mathbf{s}}(\mathbf{r})\tilde{\varphi}_{n_2}^{\mathbf{k}_{1\parallel},\mathbf{s}_1}(\mathbf{r})\\&\quad\times\bar{u}_{\mathbf{0},n_1}(\mathbf{r})u_{\mathbf{0},\tilde{S}^\mp(n_2)}(\mathbf{r})\delta(\mathbf{r}-\mathbf{R}_\eta)\mathrm{d}\mathbf{r}.\end{aligned}$$

In order to perform the above integration, we have carefully considered the delta function, $\delta(\mathbf{r}-\mathbf{R}_\eta)$. To split the fast oscillating component of the integral with respect to the smooth one is represented by the envelope function, we have assumed that the original delta function is smeared out over the volume of the Wigner-Seitz (WS) cell. Thus, $\delta(\mathbf{r}-\mathbf{R}_\eta)$ is replaced by a quasismooth step function $\delta_D(\mathbf{r}-\mathbf{R}_\eta)$ which is nonvanishing only near the $\eta^{\text{th}}$ WS cell (this approximation is studied in detail in Ref. 17). This procedure is consistent with the physical picture underlying the exchange interaction in DMS for which the hole-ion coupling takes place only inside the ionic sites. The same argument was used in Ref. 18 where the exchange coupling is assumed to have a Gaussian shape and whose parameters were chosen to fit experimental measurements. By using the Fourier decomposition

$$\tilde{\varphi}_{n_2}^{\mathbf{k}_\parallel,\mathbf{n}}(\mathbf{r})=\int\delta(\mathbf{k}_\parallel-\mathbf{k}'_\parallel)\bar{\chi}_{n_2}^{\mathbf{k}'_\parallel,\mathbf{s}}(k_z)e^{i\mathbf{k}'_\parallel\cdot\mathbf{r}+ik_zz}\mathrm{d}\mathbf{k}'_\parallel=e^{i\mathbf{k}_\parallel\cdot\mathbf{r}}\chi_{n_2}^{\mathbf{k}_\parallel,\mathbf{s}}(z),$$

the expression (29) reads

$$\begin{aligned}&\mathcal{V}^\eta_{\mathbf{k}_\parallel,\mathbf{s},m\to\mathbf{k}_{1\parallel},\mathbf{s}_1,m'}\\&\quad=\gamma\mathbf{M}^\pm_{m,m'}\sum_{n_1,n_2}S^\mp(n_2)\sum_{\mathbf{R}_l}\bar{\tilde{\varphi}}_{n_1}^{\mathbf{k}_\parallel,\mathbf{s}}(\mathbf{R}_l)\tilde{\varphi}_{n_2}^{\mathbf{k}_{1\parallel},\mathbf{s}_1}(\mathbf{R}_l)\delta_D(\mathbf{R}_l-\mathbf{R}_\eta)\\&\qquad\times\int_{cell}\bar{u}_{\mathbf{0},n_1}(\mathbf{r})u_{\mathbf{0},\tilde{S}^\mp(n_2)}(\mathbf{r})\mathrm{d}\mathbf{r}\\&\quad=\gamma\mathbf{M}^\pm_{m,m'}e^{i(\mathbf{k}_{1\parallel}-\mathbf{k}_\parallel)\cdot\mathbf{R}_\eta}\sum_{n_2}S^\mp(n_2)\bar{\chi}_{\tilde{S}^\mp(n_2)}^{\mathbf{k}_\parallel,\mathbf{s}}(R_\eta^z)\chi_{n_2}^{\mathbf{k}_{1\parallel},\mathbf{s}_1}(R_\eta^z)\\&\quad=\gamma e^{i(\mathbf{k}_{1\parallel}-\mathbf{k}_\parallel)\cdot\mathbf{R}_\eta}\sum_{n_2,n'_2}\mathbf{M}_{m,m'}\cdot\mathbf{S}_{n_2,n'_2}\bar{\chi}_{n'_2}^{\mathbf{k}_\parallel,\mathbf{s}}(R_\eta^z)\chi_{n_2}^{\mathbf{k}_{1\parallel},\mathbf{s}_1}(R_\eta^z),\end{aligned}$$

where $\mathbf{S}^\mp_{n,n'}=\delta_{n,n'\mp1}\sqrt{(\mathfrak{S}^h\mp n)(\mathfrak{S}^h\pm n+1)}$ with $\mathfrak{S}^h=3/2$. The use of the homogeneous approximation leads to

$$\begin{aligned}&|\tilde{\mathcal{V}}_{\mathbf{k}_\parallel,\mathbf{s},m\to\mathbf{k}_{1\parallel},\mathbf{s}_1,m'}|^2\\&\quad=\frac{1}{V}\int|\mathcal{V}^\eta_{\mathbf{k}_\parallel,\mathbf{s},m\to\mathbf{k}_{1\parallel},\mathbf{s}_1,m'}|^2\mathrm{d}\mathbf{R}_\eta\\&\quad=\gamma^2\frac{1}{d}\int_{-d/2}^{d/2}\left|\sum_{n_2,n'_2}\mathbf{M}_{m,m'}\cdot\mathbf{S}_{n_2,n'_2}\bar{\chi}_{n'_2}^{\mathbf{k}_\parallel,\mathbf{s}}(z)\chi_{n_2}^{\mathbf{k}_{1\parallel},\mathbf{s}_1}(z)\right|^2\mathrm{d}z.\end{aligned}$$

Finally, the scattering kernel $\mathcal{W}$ can be written as

$$\mathcal{W}_{\mathbf{s},m}=\frac{2\pi}{\hbar}N^M\gamma^2\sum_{\iota=\pm1}|\mathbf{M}^{\mathrm{sgn}(\iota)}_{m+\iota,m}|^2(1-\delta_{m,\iota\mathfrak{S}^M})\sum_{\mathbf{s}_1}\mathcal{I}^{\mathrm{sgn}(\iota)}_{m,\mathbf{s},\mathbf{s}_1},$$

where $\mathrm{sgn}(\iota)$ denotes the sign of $\iota$,

$$\begin{aligned}\mathcal{I}^{\mathrm{sgn}(\iota)}_{m,\mathbf{s},\mathbf{s}_1}=\sum_{\mathbf{k}_\parallel,\mathbf{k}_{1\parallel}}&\mathfrak{C}^{\mathrm{sgn}(\iota)}_{\mathbf{s},\mathbf{s}_1}(\mathbf{k}_\parallel,\mathbf{k}_{1\parallel})(\mathfrak{n}_{m+\iota}f_{\mathbf{s}_1}(E_{\mathbf{k}_{1\parallel}})[1-f_{\mathbf{s}}(E_{\mathbf{k}_\parallel})]\\&-\mathfrak{n}_mf_{\mathbf{s}}(E_{\mathbf{k}_\parallel})[1-f_{\mathbf{s}_1}(E_{\mathbf{k}_{1\parallel}})])\\&\times\delta(E_{m+\iota}-E_m-E_{\mathbf{s}}-E_{\mathbf{k}_\parallel}+E_{\mathbf{s}_1}+E_{\mathbf{k}_{1\parallel}}),\end{aligned}$$

and

$$\begin{aligned}&\mathfrak{C}^{\mathrm{sgn}(\iota)}_{\mathbf{s},\mathbf{s}_1}(\mathbf{k}_\parallel,\mathbf{k}_{1\parallel})\\&\quad=\frac{1}{d}\int\left|\sum_n(1-\delta_{n,-\iota\mathfrak{S}^h})\mathbf{S}^{-\mathrm{sgn}(\iota)}_{n-\iota,n}\bar{\chi}_n^{\mathbf{k}_\parallel,\mathbf{s}}(z)\chi_{n-\iota}^{\mathbf{k}_{1\parallel},\mathbf{s}_1}(z)\right|^2\mathrm{d}z.\end{aligned}$$

In the above expressions, $\mathfrak{S}^M=5/2$, $f_{\mathbf{s}}(E_{\mathbf{k}_\parallel})$ is the Fermi-Dirac function for an energy $E_{\mathbf{s}}+E_{\mathbf{k}_\parallel}$ and $\mu_{\mathbf{s}}$ is an out-of-equilibrium chemical potential. The energy $E_m$ of the $m^{\text{th}}$

ionic level is obtained by using the Zener mean-field interaction. In the axial approximation $[\mathcal{H}_{kp}(\mathbf{k}_\parallel, \frac{\partial}{\partial z})]$ depends on $\mathbf{k}_\parallel$ only trough $|\mathbf{k}_\parallel|e^{i\phi}$ where $\phi$ is the angle between $\mathbf{k}_\parallel$ and the $x$ axis[9,19] and therefore, $\mathfrak{C}(\mathbf{k}_\parallel, \mathbf{k}'_\parallel) = \mathfrak{C}(|\mathbf{k}_\parallel|, |\mathbf{k}'_\parallel|)$ (this is true only up to the second order in $k$). Finally, for a two-dimensional system, we have

$$\mathcal{I}^{\mathrm{sgn}(\iota)}_{m,\mathbf{s},\mathbf{s}_1} = m^*_s m^*_{s_1} \left(\frac{2\pi V}{\hbar^2}\right)^2 \int_{\max\{0,-\Delta^{m+\iota,\mathbf{s}_1}_{m,\mathbf{s}}\}}^{\infty} \mathfrak{C}^{\mathrm{sgn}(\iota)}_{\mathbf{s},\mathbf{s}_1}$$
$$\times [F_s(E+\Delta^{m+\iota,\mathbf{s}_1}_{m,\mathbf{s}}), F_{s_1}(E)](\mathfrak{n}_{m+\iota} f_{\mathbf{s}_1}(E)$$
$$\times [1 - f_{\mathbf{s}}(E+\Delta^{m+\iota,\mathbf{s}_1}_{m,\mathbf{s}})] - \mathfrak{n}_m f_{\mathbf{s}}(E+\Delta^{m+\iota,\mathbf{s}_1}_{m,\mathbf{s}})$$
$$\times [1 - f_{\mathbf{s}_1}(E)])\mathrm{d}E,$$

where $F_s(E) = 2m^*_s\sqrt{E}$, with an effective electron mass $m^*_s$ and $\Delta^{m',\mathbf{s}'}_{m,\mathbf{s}} = E_{\mathbf{s}'} + E_{m'} - E_{\mathbf{s}} - E_m$.

## III. NUMERICAL RESULTS

Equations (23)–(25) have been solved in order to study the role played by the quantum confinement and the hole density on the dynamical evolution of the total magnetization after laser irradiation. We have considered a DMS sample composed of a $Ga_{0.925}Mn_{0.075}As$ layer deposited on a GaAs buffer layer and a semi-insulating GaAs substrate. The initial hole and magnetic-ion distributions are calculated using the stationary mean-field Zener model.[16] The laser pulse excitation is assumed to take place at $t=0^+$. Details and justifications based on physical grounds of the excited hole density used in the calculation are given in Refs. 5 and 6. In all simulations the thickness $w$ of the doped layer varies within the range 4–6 nm, $\gamma = 0.09$ eV nm$^3$ and $m^*_s = 0.067\ m_0$.[16]

In Figs. 3–5, the miniband diagrams calculated by using the Zener mean-field theory are depicted. In Fig. 3, a $w = 6$ nm DMS sample without Mn doping and having a background hole density $n^h \equiv \Sigma_{\mathbf{s}} n_{\mathbf{s}} = 10^{-4}$ nm$^{-3}$ is considered. In all the figures, the $z$ axis corresponds to the confinement direction of the hole gas coming from the abrupt junction between the DMS active Mn-doped region and the insulating layers. The $x-y$ plane represents the free parallel directions

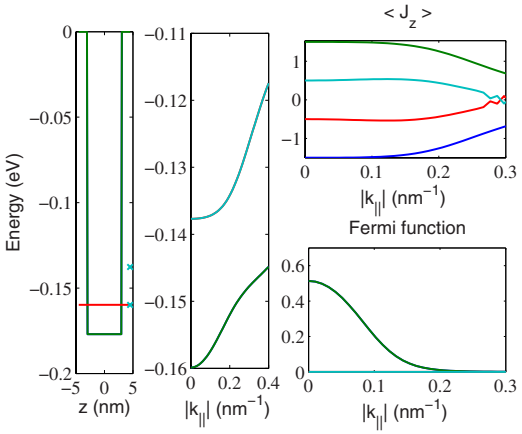


FIG. 3. (Color online) Band diagram of a 6 nm GaAs quantum well without Mn magnetic ions (see text for the meaning of the different panels). The density of holes is $n^h = 10^{-4}$ nm$^{-3}$ and the temperature $T^h = 10$ K.

of motion for the holes. On the left panel of Figs. 3–5, the self-consistent hole band edge profile is represented (the Coulomb repulsion between the holes is taken into account by using the standard mean-field Hartree approximation). The horizontal line denotes the position of the hole chemical potential and the crosses represent the energies of the resonant levels (which correspond to the $\mathbf{k}_\parallel = \mathbf{0}$ energy values of the various minibands). On the central panel, the steady state miniband diagram (here each miniband is twofold degenerated) for a temperature $T^h = 10$ K is depicted. On the upper right panel, the expectation value of the hole total angular momentum $\langle J_z \rangle$ is shown as a function of $|\mathbf{k}_\parallel|$. For $|\mathbf{k}_\parallel| \neq 0$ the off-diagonal components of the $kp$ Hamiltonian mix the heavy- and light-hole components of the eigenstates and therefore the $z$ component of the hole-spin polarization is reduced. On the lower right panel, the occupation probability of the different bands is represented: the figure shows that, for a temperature of 10 K and a hole density of $10^{-4}$ nm$^{-3}$, only two (degenerate) minibands are populated. Furthermore, a comparison of $\langle J_z \rangle$ reported on the upper right panel shows that the contribution of the hole with parallel momentum greater than 0.1 nm$^{-1}$ (where the heavy and hole com-

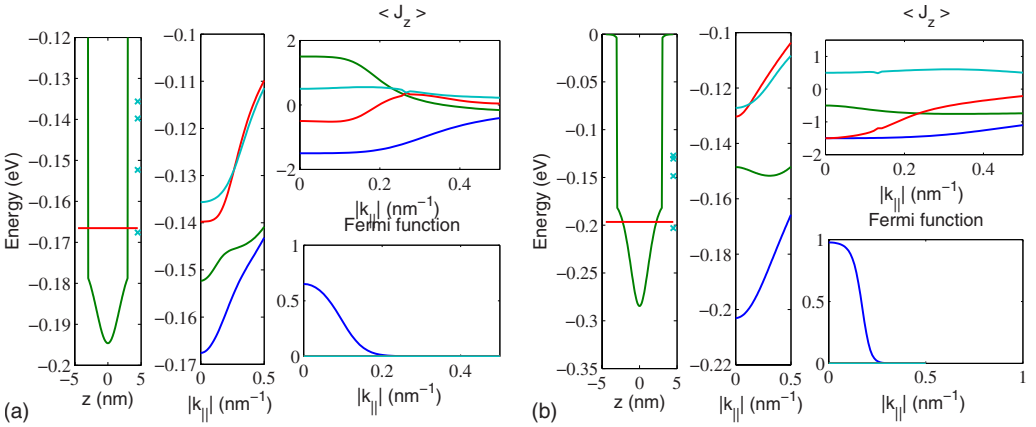


FIG. 4. (Color online) Band diagram of a 6 nm $Ga_{0.925}Mn_{0.075}As$ quantum well. The background hole density is: (a) $n^h = 10^{-4}$ nm$^{-3}$, (b) $n^h = 5 \cdot 10^{-4}$ nm$^{-3}$. The temperature is $T^h = 10$ K.

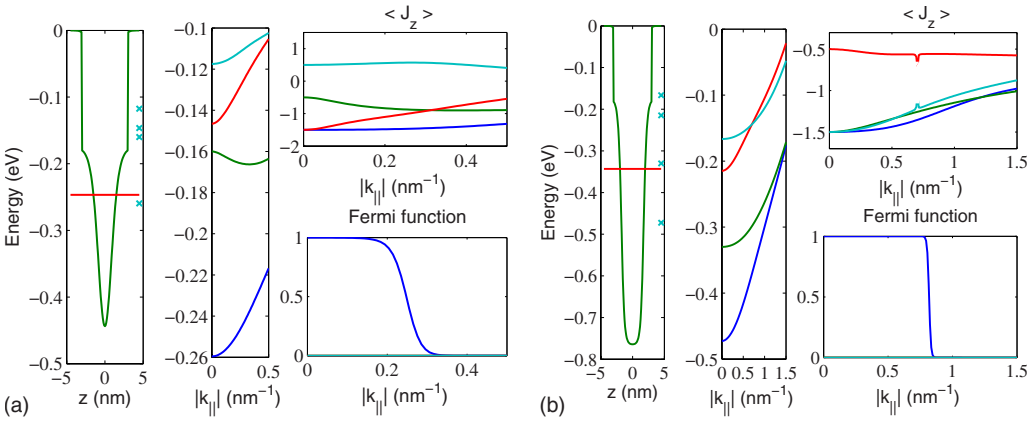


FIG. 5. (Color online) Band diagram of a 6 nm $Ga_{0.925}Mn_{0.075}As$ quantum well. The background hole density is: (a) $n^h=10^{-3}$ nm$^{-3}$, (b) $n^h=10^{-2}$ nm$^{-3}$. The temperature is $T^h=10$ K.

ponents mix together) gives a non-negligible contribution to the total spin polarization of the hole gas. As a consequence, the smearing of the hole distribution around $|\mathbf{k}_\parallel|=0$ cannot be discarded and the hole-spin projection along the $z$ axis cannot be considered as a good quantum number.

In Fig. 4 and 5, we show, for different values of the hole density, the modification of the miniband diagrams when the Mn doping is included. The numerical results reveal that the band characteristics (minimum, shape, and expectation value of the spin eigenstates) are strongly affected by the hole concentration. Therefore, we also expect that the dynamical evolution of the total magnetization will be modified (may be characterized by different time scales) when the doping concentration and the layer thickness $w$ of the sample are varied. In Fig. 6, we show the static magnetization as a function of temperature, obtained by using the mean-field Zener model. In particular, we represent the expectation value of the hole spin $\langle S_z\rangle$ (which lies in the interval $[-0.5,0.5]$) which is typically preferred to the total angular momentum $\langle J_z\rangle$ for representing the static magnetization curves (see, for example, Ref. 16). As already mentioned, the equilibrium values of the magnetization define the initial distributions that are used in the dynamical simulations. In particular, the equilibrium ion (panel $a$) and hole (panel $b$) magnetization for different hole background densities are represented.

In Fig. 7 and 8, the time evolution of the total magnetization for different sample thicknesses is presented. The laser excitation takes place at $t=0^+$ and according to the discussion of Ref. 6 its main effect is to raise instantaneously the initial temperature of the hole gas. In Fig. 7 and 8, the initial temperature is $T^h=10$ K and the corresponding temperature of the excited hole gas is 20 K. Thus, we are considering a very weak laser excitation regime, which does not notably modify the self-consistent band structure calculated at equilibrium. Numerical results show that our model is able to reproduce the initial ultrafast lowering of the total magnetization of the sample and the subsequent recovery of the equilibrium state. In particular, the characteristic times of these processes are strongly affected both by the hole background density and the sample thickness. This is clearly illustrated in Fig. 9 where we have represented the time $t_m$ (panel $a$) corresponding to the minimum of the differential magnetization $\delta M(t)=\frac{M_{\rm tot}(t)-M_{\rm tot}(0)}{M_{\rm tot}(0)}$ where $M_{\rm tot}=\langle M_z\rangle N^M+\langle S_z\rangle n^h$ and its maximum value, $\delta M_m\equiv\delta M(t_m)$ (panel $b$) for different hole background densities. The results are represented in logarithmic scale and show, within the range of the hole concentration $10^{-4}-10^{-2}$ nm$^{-3}$ considered in this work, a nearly power-law decrease in the demagnetization time $t_m$ and a saturation of $\delta M_m$ as $n^h$ increases. In order to understand the above behavior a detailed analysis of the miniband characteristics and the scalar product of in and out scattering states would be required. As a general remark, we note that the rising of the hole density leads to the occupation of higher $|\mathbf{k}_\parallel|$ states where the $z$ component of the hole spin is not a good quantum number. Due to the coupling to the in-plane spin component, this higher energetic population accelerates the dissipation processes of the total spin. On the other hand, the increase in the hole concentration allows the access to a new miniband higher in energy where the minimum energy

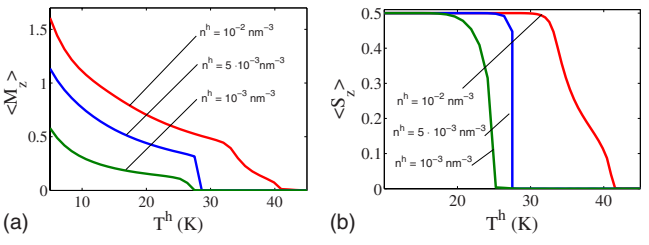


FIG. 6. (Color online) Magnetic ion (a) and hole (b) static magnetization as a function of temperature for different values of the background hole density. The thickness of the sample is $w=6$ nm.

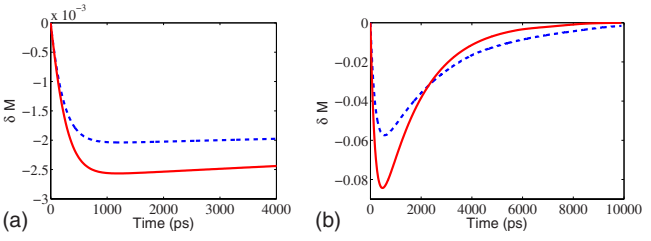


FIG. 7. (Color online) Time evolution of the normalized quantity $\delta M(t)=\frac{M_{\rm tot}(t)-M_{\rm tot}(0)}{M_{\rm tot}(0)}$ for different sample thicknesses and hole background densities: (a) $n^h=10^{-4}$ nm$^{-3}$; (b) $n^h=5\times10^{-4}$ nm$^{-3}$. Layer thickness $w=6$ nm (full lines) and $w=4$ nm (dashed lines).

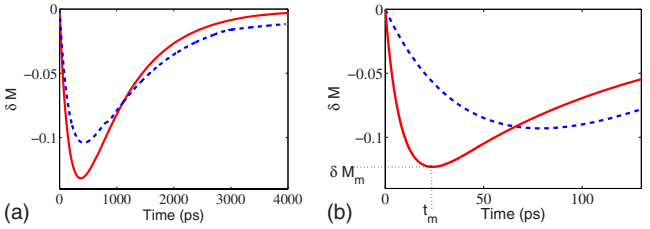


FIG. 8. (Color online) Same as Fig. 7 with: (a) $n^h=10^{-3}$ nm$^{-3}$ and (b) $n^h=10^{-2}$ nm$^{-3}$. The quantities $t_m$ and $\delta M_m$ are displayed on panel (b).

states are around the $|\mathbf{k}_\parallel|=0$ point (which are, in the present model, stable against the spin Elliot-Yafet dispersion processes) and which can justify a partial saturation of the demagnetization processes. Moreover, during the demagnetization processes it is possible to define a time-dependent quasiequilibrium temperature for the ion impurities. When the system is excited, the hole temperature is instantaneously raised form 10 to 20 K. The laser excitation does not affect directly the ion spins so that the total dispersion of the ion spins for $t=0^+$ coincide with the usual spin distribution of a paramagnetic system at a lattice temperature of 10 K. During the evolution, the exchange interaction generates a heat flux from the hole gas to the ions. Even though this mechanism is not able to completely equilibrate the hole temperature with that of the ions (as shown by the numerical solution, the ion temperature rises up to nearly 13 K), when the hole density increase, the temperature of the ion spins is more efficiently driven toward the hole temperature. Since the total magnetization of the sample is essentially equivalent to the ion magnetization (this is due to the difference between hole and Mn concentration) a saturation of the total demagnetization is expected when the ion temperature reaches the initial hot hole temperature.

Our model *is free of any phenomenological parameters* which force the spin of the holes to relax. As described in Sec. II A, hole-spin relaxation comes from the entanglement between the spin direction and the linear momentum of the hole, which gives rise to a mixing of the hole-spin components.

The hypothesis of a quasiequilibrium Fermi distribution for the momentum dispersion of the hole gas in presence of a complex band structure like those of Fig. 4 and 5 resolves in a fast thermalization of the initial spin configuration. The 6 nm sample with a background hole concentration of $10^{-3}$ nm$^{-3}$ provides a simple case for understanding the details of the spin relaxation processes.

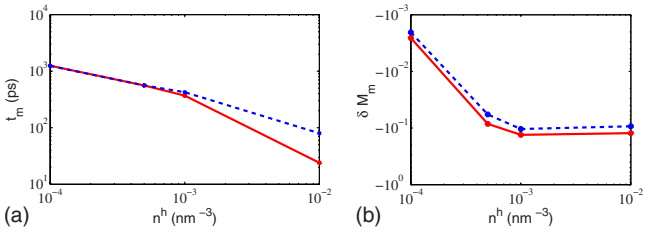


FIG. 9. (Color online) $t_m$ (a) and as a function of $n^h$; (b) $\delta M_m$ as a function of $n^h$. Logarithmic axis scales are used. Layer thickness $w=6$ nm (full lines) and $w=4$ nm (dashed lines).

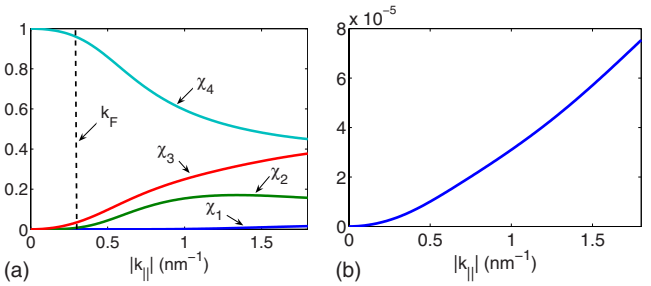


FIG. 10. (Color online) (a) $z$ integral of $|\chi_n^{|\mathbf{k}_\parallel|,-3/2}|^2$ with $n=1,\ldots,4$. The dashed vertical line denotes the position of the Fermi momentum. (b) Transition rate $\mathfrak{C}^+_{3/2,3/2}(k_F,|\mathbf{k}_\parallel|)$ as a function of the outgoing momentum $|\mathbf{k}_\parallel|$.

In fact, as can be clearly seen in Fig. 5(a), before the laser excitation only the first heavy hole band $|3/2;-3/2\rangle$ is populated (the occupation probability for $T^h=10$ K is plotted on the bottom right panel). The first available higher energy band is the $|3/2;-1/2\rangle$ light-hole miniband [for the band classification, see the upper right panel of the hole total angular momentum $\langle J_z\rangle$ in Fig. 5(a)]. Despite the fact that the direct transition $|3/2;-3/2\rangle\rightarrow|3/2;-1/2\rangle$, which is a consequence of the hole-ion scattering process of type $m\rightarrow m+1$ is possible, the large energy gap (nearly 0.1 eV) between the two bands strongly reduces this process. The main hole-spin relaxation channel is therefore an intraband process. Indeed, for $|\mathbf{k}_\parallel|=0$ the envelope function $\chi_n^{|\mathbf{k}_\parallel|=0,s=-3/2}(z)$ has a single component $n=s$ which corresponds to a spin-down state. For $|\mathbf{k}_\parallel|=k_F$, where $k_F$ denotes the Fermi momentum, the eigenstate becomes a mixture of spin-up and spin-down states. This can be seen in Fig. 10(a) where the $z$-integral of $|\chi_n^{|\mathbf{k}_\parallel|,-3/2}|^2$ with $n=1,\ldots,4$ and for different values of $|\mathbf{k}_\parallel|$ are depicted. The Fermi level is marked by a vertical line. In order to illustrate the spin transition, let us consider an ion spin transition from $m=1/2$ to $m'=-1/2$. The numerical solution shows that the energy difference of the ionic levels is $\Delta_m^{m'}\simeq 1.3\times 10^{-4}$ eV and corresponds to a momentum difference of the scattered holes of $\Delta|\mathbf{k}_\parallel|\simeq 0.02$ nm$^{-1}$ with a transition rate given by $\mathfrak{C}^+_{3/2,3/2}$. In particular, a hole-spin transition between the fourth component of the incoming hole $|3/2;-3/2\rangle=1/\sqrt{2}|X-iY;\downarrow\rangle$ and the second component of the outgoing particle $|3/2;-1/2\rangle=-1/\sqrt{6}|X-iY;\uparrow\rangle-\sqrt{2/3}|Z;\downarrow\rangle$ is allowed. As a consequence of this transition and according to the hypothesis of the hole gas thermalization, in an intraband Kondo-like process the spin of the system is not conserved. In fact, a spin lowering of the ions does not correspond to a net increase in the hole-spin gas. This is due to the fact that, in our model, the total spin polarization of each miniband is a function of the hole temperature and density which are both constant in such interband transitions. Our findings agree with the physical picture outlined in Ref. 10 where a confined $Zn_{1-x}Mn_xSe/Zn_{1-y}Be_ySe$ structure has been considered. Due to the giant Zeeman splitting, in a low temperature regime, the initial and final states of the holes belong to the same spin sub-band and nonzero matrix elements of the hole-spin operator in the Luttinger Hamiltonian leads to a mixing between the heavy and light components of the hole states.

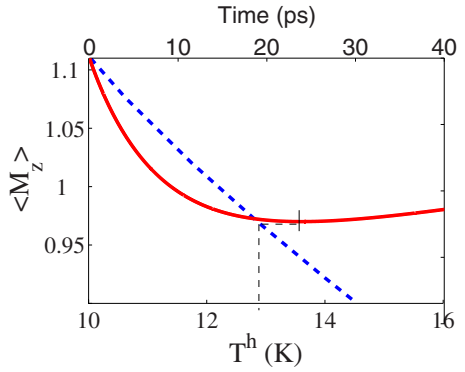


FIG. 11. (Color online) Ion magnetization as a function of time (full line and up horizontal axis) and static value of the ion magnetization at equilibrium as a function of temperature (dashed line and down horizontal axis). The hole background density is $n^h = 10^{-2}$ nm$^{-3}$.

In Fig. 10(a), the value of the transition rate $\mathfrak{C}^+_{3/2,3/2}(k_F, |\mathbf{k}_\parallel|)$ as a function of the outgoing momentum $|\mathbf{k}_\parallel|$ is shown. Let us note that a transition toward $|\mathbf{k}_\parallel| = 0$ is forbidden since the spin of the scattered particle is raised which is not allowed when the final state is $\chi_n^{|\mathbf{k}_\parallel|=0,s=-3/2}(z)$ for which the spin is minimum.

Finally, in Fig. 11, we report the time evolution of the ion magnetization (full line and top horizontal axis) and the static value of the magnetization at equilibrium as a function of temperature (dashed line and down horizontal axis). The comparison between this two quantities shows that, despite the fact that the laser excitation raises the hole temperature up to 20 K, the energy flux between the holes and the ions is not efficient enough to destroy the original spin order and to bring the system up to the 20 K equilibrium configuration. The minimum of the magnetization is reached after nearly 20 ps and corresponds to an equilibrium temperature of nearly 13 K.

## IV. CONCLUSIONS

In this work, we have developed a dynamical model able to explain the observed time evolution of the magnetization in thin diluted magnetic semiconductor quantum wells and, in particular, the phenomenon of ultrafast demagnetization that takes place within a picosecond time scale. The microscopic mechanism underlying this effect is related to the hole-spin relaxation produced by the Elliot-Yafet mechanism and the mixing between heavy- and light-hole bands. We showed that the quantum confinement and the hole background density play an important role on the time evolution of the total magnetization. Besides the hole background density, the magnetic doping concentration would also affect the time evolution of the total magnetization. Theoretical predictions have been obtained for 4 and 6 nm GaMnAs samples. Finally, let us stress that our approach is free of any parameters and therefore goes well beyond previous works based on more phenomenological grounds.

## ACKNOWLEDGMENTS

We thank P. Gilliot, M. Gallart, and J. Besbas for helpful discussions and we acknowledge financial support from the French National Research Agency ANR (Project No. ANR-06-BLAN-0059).

[1] E. Beaurepaire, J.-C. Merle, A. Daunois, and J.-Y. Bigot, Phys. Rev. Lett. **76**, 4250 (1996).
[2] H. Ohno, Science **281**, 951 (1998).
[3] T. Dietl, H. Ohno, F. Matsukura, J. Cibert, and D. Ferrand, Science **287**, 1019 (2000).
[4] J. Wang, C. Sun, J. Kono, A. Oiwa, H. Munekata, Ł. Cywiński, and L. J. Sham, Phys. Rev. Lett. **95**, 167401 (2005).
[5] Ł. Cywiński and L. J. Sham, Phys. Rev. B **76**, 045205 (2007).
[6] O. Morandi, P.-A. Hervieux, and G. Manfredi, New J. Phys. **11**, 073010 (2009).
[7] R. J. Elliott, Phys. Rev. **96**, 266 (1954).
[8] G. P. Zhang and T. F. George, Phys. Rev. B **78**, 052407 (2008).
[9] R. Ferreira and G. Bastard, Phys. Rev. B **43**, 9687 (1991).
[10] A. V. Akimov, A. V. Scherbakov, D. R. Yakovlev, I. A. Merkulov, M. Bayer, A. Waag, and L. W. Molenkamp, Phys. Rev. B **73**, 165328 (2006).
[11] R. Winkler, *Spin-Orbit Coupling Effects in Two-Dimensional Electron and Hole Systems, Springer Tracts in Modern Physics* (Springer, Berlin, 2003), Vol. 191.
[12] B. König, I. A. Merkulov, D. R. Yakovlev, W. Ossau, S. M. Ryabchenko, M. Kutrowski, T. Wojtowicz, G. Karczewski, and J. Kossut, Phys. Rev. B **61**, 16870 (2000).
[13] B. Lee, T. Jungwirth, and A. H. MacDonald, Phys. Rev. B **61**, 15606 (2000).
[14] G. Bastard, Phys. Rev. B **24**, 5693 (1981).
[15] B. A. Foreman, Phys. Rev. B **48**, 4964 (1993).
[16] N. Kim, H. Kim, J. W. Kim, S. J. Lee, and T. W. Kang, Phys. Rev. B **74**, 155327 (2006).
[17] B. A. Foreman, Phys. Rev. B **52**, 12241 (1995).
[18] L. Brey and G. Gómez-Santos, Phys. Rev. B **68**, 115206 (2003).
[19] Calvin Yi-Ping Chao and S. L. Chuang, Phys. Rev. B **46**, 4110 (1992).